Interstellar extinction toward MWC 148

R. Zamanov[1], I. Stateva[1], J. Marti[2], K. Stoyanov[1], V. Marchev[1]

[1] Institute of Astronomy and National Astronomical Observatory, Bulgarian Academy of Sciences, Tsarigradsko Shose 72, BG-1784 Sofia, Bulgaria

[2] Departamento de Física, Escuela Politécnica Superior de Jaén, Universidad de Jaén, Campus Las Lagunillas, A3, 23071, Jaén, Spain

e-mails: stateva@astro.bas.bg, kstoyanov@astro.bas.bg

(Submitted on 01.04.2025; accepted on 07.05.2025)

Abstract. We analyse high resolution optical spectra of MWC 148 (optical counterpart of the γ-ray source HESS J0632+057) obtained at Observatoire de Haute Provence and Rozhen Observatory in order to better determine the interstellar extinction toward MWC 148. We use the relations between the equivalent widths of the Diffuse Interstellar Bands and the interstellar extinction in optical wavelengths. We measure equivalent widths of 7 diffuse interstellar bands and estimate the interstellar extinction to be $E_{B-V} = 0.85 \pm 0.08$.

Key words: Stars: emission-line, Be – binaries: spectroscopic – Gamma rays: stars – Stars: individual: MWC 148, HESS J0632+057

1 Introduction

MWC 148 (HD 259440, BD+05 1291) was identified as the counterpart of the variable TeV source HESS J0632+057 (Aharonian et al. 2007, Aragona et al. 2010; Matchett & van Soelen 2025). HESS J0632+057 belongs to a rare subclass of binary systems that emit γ-rays above 100 GeV. The optical counterpart of HESS J0632+057 is the Be star MWC 148, which, through *Gaia* EDR3 parallaxes (Gaia Collaboration et al. 2021) was estimated to be at a distance of 1759 ± 90 pc (Bailer-Jones et al. 2021). It is a binary system consisting of a Be star and a compact object. The secondary can be a neutron star or a black hole. The orbital period is 317.3 ± 0.7 days, obtained with a refined analysis of X-ray data (Adams et al. 2021). There is also a modulation of the very high-energy γ-ray fluxes with a similar period 316.7 ± 4.4 days. Its high-energy light curve features a sharp primary peak and broader secondary peak (Tokayer et al. 2021). The optical emission lines of MWC 148 are almost identical to those of the well-known Be star γ Cas (Zamanov et al. 2016), which indicates that the circumstellar discs and the orbital periods are comparable.

Interstellar extinction is a key factor in determining the physical parameters of MWC 148. Estimates of the extinction toward this object vary significantly. The NASA/NED extinction calculator (Madore et al. 1992) provides an upper limit of $E_{B-V} \leq 0.6$ magnitude, while the GAIA DR3 (Gaia Collaboration et al. 2021) reports a considerably higher value of $E_{B-V} = 1.090$. In this study, we analyze diffuse interstellar bands (DIBs) observed in high-resolution optical spectra to derive an independent estimate of the interstellar extinction toward MWC 148.

2 Observations

In this study we use five optical spectra obtained with the SOPHIE spectrograph (Perruchot et al. 2008) mounted on the 1.93m telescope of the Haute-

Table 1. Journal of spectral observations of MWC 148. In the columns are given the observatory, date, UT of the start of the exposure, the exposure time, and signal-to-noise ratio around 6600 Å.

#	observatory spectrograph	date-obs	exposure	S/N
#1	OHP SOPHIE	2011-11-23 03:41	60 min	160
#2	OHP SOPHIE	2011-12-08 00:26	60 min	145
#3	OHP SOPHIE	2011-12-21 00:50	60 min	150
#4	OHP SOPHIE	2011-12-29 00:55	60 min	110
#5	OHP SOPHIE	2012-01-03 00:22	60 min	140
#6	Rozhen ESpeRo	2022-04-14 19:04	40 min	45
#7	Rozhen ESpeRo	2024-02-27 18:23	90 min	40
#8	Rozhen ESpeRo	2024-01-22 19:02	45 min	55

Table 2. Equivalent widths of DIBs in the spectra of MWC 148. The last row gives the full width of the half maximum (FWHM) for each DIB.

#	EW_{5780} [Å]	EW_{5797} [Å]	EW_{6614} [Å]	EW_{6270} [Å]	EW_{6379} [Å]	EW_{5850} [Å]	EW_{6196} [Å]
#1	0.3425	0.1444	0.1706	0.0630	0.1020	0.0656	0.0353
#2	0.3166	0.1379	0.1696	0.0555	0.1061	0.0604	0.0354
#3	0.3074	0.1563	0.1746	0.0501	0.1015	0.0695	0.0353
#4	0.2887	0.1278	0.1719	0.0647	0.1038	0.0681	0.0422
#5	0.3102	0.1405	0.1876	0.0756	0.0941	0.0688	0.0405
#6	0.3345	0.1517	0.174				
#7	0.3328	0.1420	0.157				
#8	0.3424	0.1491	0.164				
FWHM [km s^{-1}]	107 ± 2	38 ± 1	42 ± 1	49 ± 2	26 ± 1	40 ± 2	20 ± 1

Table 3. Estimated E_{B-V} from EWs of DIBs in the spectra of MWC 148: (1) using ODR and (2) OLS fitting of Puspitarini et al. (2013).

DIB	E_{B-V} (1)	E_{B-V} (2)
DIB 5780	0.73 ± 0.04	0.78 ± 0.05
DIB 5797	0.91 ± 0.07	0.81 ± 0.06
DIB 6614	0.89 ± 0.04	0.90 ± 0.04
DIB 6270	0.95 ± 0.15	0.75 ± 0.11
DIB 6379	1.06 ± 0.05	0.99 ± 0.04
DIB 5850	0.83 ± 0.05	0.76 ± 0.04
DIB 6196	0.99 ± 0.09	0.74 ± 0.07
average	0.909 ± 0.108	0.820 ± 0.092

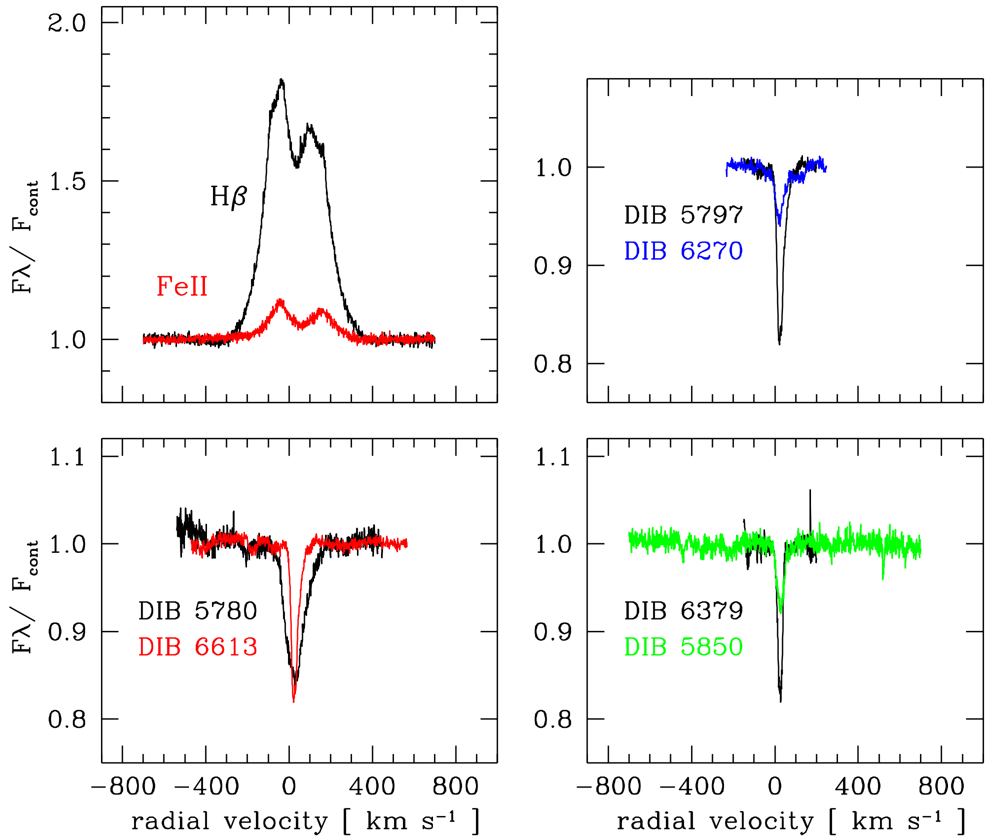

Fig. 1. Profiles of the $H\beta$ and FeII 5316 emission lines together with diffuse interstellar bands DIB 5780, 6613, 5797, 6270, 6379, 5850.

Provence Observatory (OHP), France. The spectra used in this study were selected from the SOPHIE Archive based on their long exposure times and high signal-to-noise (S/N) ratios, ensuring high-quality data suitable for detailed analysis and minimizing measurement uncertainties. The spectra are downloaded from the SOPHIE Archive which gives access to the observations obtained with the spectrograph since it started operations in August 2006. Additionally, three spectra have been secured with the ESpeRo echelle spectrograph (Bonev et al. 2017) mounted on the 2.0m RCC telescope of the Rozhen National Astronomical Observatory, Bulgaria. The SOPHIE spectrograph has a resolution of $\sim$ 75 000 and ESpeRo – of $\sim$ 30 000. Journal of observations is given in Table 1.

In the SOPHIE spectra we identified 12 DIBs – 5780.38 Å, 5797.06 Å, 6613.62 Å, 6269.85 Å, 6379.32 Å, 5849.81 Å, 6195.98 Å, 4726.83 Å, 4762.61 Å, 4963.88 Å, 6660.71 Å, 6699.32 Å. The equivalent widths (EWs) of seven of them were measured with good (better than ±10%) accuracy. From the Rozhen spectra we were able to measure the EWs of three DIBs. The measurements are presented in Table 2, with typical uncertainties ranging from 5% to 10%. The obtained variations in equivalent widths (EWs) across different epochs are attributed to measurement errors. Given the critical role of spectral resolution and signal-to-noise ratio in ensuring measurement accuracy, we rely on the high S/N spectra obtained with the SOPHIE spectrograph.

3 Results

For each diffuse interstellar band (DIB), the local continuum was fitted using a spectral region of approximately 20 Å. The equivalent widths (EWs) of the DIBs were measured using the *splot* routine of *IRAF*. The profiles of the DIBs are shown in Fig. 1. For illustrative comparison, the profiles of the Hβ and FeII 5316 emission lines are also included. These emission lines, among the most prominent in the spectrum, are shown to emphasize their different origin: they are formed in the circumstellar disc, whereas the DIBs originate in the interstellar medium. Table 2 also lists the full width at half maximum (FWHM) of the DIBs, derived through Gaussian fitting.

To calculate the interstellar extinction we use the results in Puspitarini et al. (2013), where the relations between the EWs of the DIBs and the interstellar extinction E_{B-V} are given. We will use them in the following forms:

$$E_{B-V} = 0.0006 + 2.5\ EW_{5780} \tag{1}$$

$$E_{B-V} = 0.0086 + 2.3\ EW_{5780} \tag{2}$$

$$E_{B-V} = 0.0291 + 5.5\ EW_{5797} \tag{3}$$

$$E_{B-V} = 0.0203 + 6.3\ EW_{5797} \tag{4}$$

$$E_{B-V} = 0.0051 + 5.1\ EW_{6614} \tag{5}$$

$$E_{B-V} = 0.0008 + 5.1\ EW_{6614} \tag{6}$$

$$E_{B-V} = 0.0051 + 5.1\ EW_{6270} \tag{7}$$

$$E_{B-V} = 0.0008 + 5.1\ EW_{6270} \tag{8}$$

$$E_{B-V} = 0.0383 + 9.4\ EW_{6379} \tag{9}$$

$$E_{B-V} = 0.0359 + 10.1\ EW_{6379} \tag{10}$$

$$E_{B-V} = -0.0073 + 11.6\ EW_{5850}, \tag{11}$$

$$E_{B-V} = -0.0163 + 12.7\ EW_{5850}, \tag{12}$$

$$E_{B-V} = -0.0277 + 20.4\ EW_{6196} \tag{13}$$

$$E_{B-V} = -0.0349 + 21.7\, EW_{6196} \tag{14}$$

In the equations above, all equivalent widths (EWs) are expressed in Ångströms. The values used are the average EWs listed in Table 2. For each DIB, two empirical relations are available — one based on ordinary least squares (OLS) fitting and the other on orthogonal distance regression (ODR) — both taken from Table 2 of Puspitarini et al. (2013). We adopt the coefficients marked with an asterisk (*), which correspond to fits excluding peculiar objects. The resulting estimates of E_{B-V} for each DIB are presented in Table 3. Notably, the ODR-based coefficients yield extinction values approximately 10% higher than those derived using OLS. Using the ODR coefficients, we obtain $E_{B-V} = 0.911 \pm 0.104$, while the OLS coefficients give $E_{B-V} = 0.822 \pm 0.088$. Taking into account the uncertainties of both methods, we adopt a final estimate of the interstellar extinction toward MWC 148 as$E_{B-V} = 0.850 \pm 0.08$.

4 Discussion

When observing astronomical objects, it is essential to account for interstellar extinction — the absorption and scattering of radiation by dust and gas along the line of sight between the source and the observer. The degree of extinction varies depending on the object's location and the quantity and density of interstellar material, such as dust clouds, between the object and Earth.

For the interstellar extinction toward MWC 148 NASA/NED extinction calculator gives $E_{B-V} \leq 0.6$. This value is obtained on the base of the Galactic dust reddening maps provided by Schlafly & Finkbeiner (2011). Green et al. (2019) and Lallement et al. (2019) give a similar result $E_{B-V} \leq 0.5$. These catalogues are 3D maps of the interstellar dust reddening and are based on the Pan-STARRS 1 and 2MASS colours ranging wavelengths from 400 to 2400 nm. From another side a few recent catalogues give a considerably larger value $E_{B-V} = 0.854 \pm 0.066$ (Paunzen et al. 2024), $E_{B-V} = 0.865$ (Chen et al. 2019), $E_{B-V} = 1.090$ (Gaia Collaboration et al. 2021). The catalogue of Paunzen et al. (2024) gives reddening estimations based on the classical photometric indices in the Geneva, Johnson, and Strömgren-Crawford photometric systems. Chen et al. (2019) estimate the reddening using a 3D interstellar dust reddening map of the Galactic plane based on Gaia DR2, 2MASS and WISE photometry covering the wavelength range 400 to 2400 nm. The Gaia DR3 catalogue presented in Gaia Collaboration et al. (2021) uses low-resolution spectra that cover a wide range of extinction values.

Our estimation for the extinction toward MWC 148 ($E_{B-V} = 0.850 \pm 0.08$) based on the EWs of seven DIBs is in a good agreement with the values of Paunzen et al. (2024) and Chen et al. (2019). Our value does not correspond to some values obtained by using the interstellar dust reddening. Possible reasons for the discrepancy could be that (1) the interstellar medium is peculiar in the direction toward MWC 148, and/or (2) part of the DIBs visible in the spectra of MWC 148 are not formed in the interstellar dust but in the interstellar gas or in the circumstellar environment – e.g. Be circumstellar disc, circumbinary material, etc.

Conclusions: Using high resolution optical spectra obtained at the Observatoire de Haute Provence and the Rozhen Observatory, we measured the equivalent widths of seven diffuse interstellar bands (DIBs) and estimated the interstellar extinction toward MWC 148 to be $E_{B-V} = 0.85 \pm 0.08$. Our results, derived from spectroscopic analysis, are in good agreement with those reported by Paunzen et al. (2024) based on optical photometry.

Acknowledgments: This work is partly supported by grant "Studying the Outflows of High-Energy Sources: an observational multi-wavelength approach" (PID2022-136828NB-C42 funded by the Spanish MCIN/AEI/ 10.13039/501100011033) and by National Roadmap for Scientific Infrastructure coordinated by Ministry of Education and Science of Bulgaria.

The authors are very grateful to the referee for the valuable comments that helped us to improve the manuscript.

References

Adams, C. B., Benbow, W., Brill, A., et al. 2021, ApJ, 923, 241
Aharonian, F. A., Akhperjanian, A. G., Bazer-Bachi, A. R., et al. 2007, A&A, 469, L1
Aragona, C., McSwain, M. V., & De Becker, M. 2010, ApJ, 724, 306
Bailer-Jones, C. A. L., Rybizki, J., Fouesneau, M., Demleitner, M., & Andrae, R. 2021, AJ, 161, 147
Bonev, T., Markov, H., Tomov, T., et al. 2017, Bulgarian Astronomical Journal, 26, 67 (arXiv:1612.07226)
Chen, B.-Q., Huang, Y., Yuan, H.-B., et al. 2019, MNRAS, 483, 4277
Gaia Collaboration, Brown, A. G. A., Vallenari, A., Prusti, T., 2021, A&A, 649, A1
Green, G. M., Schlafly, E., Zucker, C., Speagle, J. S., Finkbeiner, D. 2019, ApJ, 887, 93
Lallement, R., Babusiaux, C., Vergely, J. L., et al. 2019, A&A, 625, A135
Paunzen E., Netopil M., Prisegen M. et al. 2024, A&A, 689, A270
Perruchot, S., Kohler, D., Bouchy, F., et al. 2008, SPIE Conference Series, 7014, 70140J
Puspitarini, L., Lallement, R., & Chen, H.-C. 2013, A&A, 555, A25
Schlafly, E. F. & Finkbeiner, D. P. 2011, ApJ, 737, 103
Tokayer, Y. M., An, H., Halpern, J. P., et al. 2021, ApJ, 923, 17
Matchett, N. & van Soelen, B. 2025, MNRAS, 536, 166
Madore, B. F., Helou, G., Corwin, H. G., et al. 1992, ASP Conf., 25, 47
Zamanov, R., Stoyanov, K., & Martí, J. 2016, Bulgarian Astronomical Journal, 24, 40 (arXiv:1509.04191)